

Young's Modulus Measurement Using a Simplified Transparent Indenter Measurement Technique

C. Feng · B.S. Kang

Received: 22 October 2006 / Accepted: 16 July 2007 / Published online: 9 August 2007
© Society for Experimental Mechanics 2007

Abstract In material nano- and micro-indentation research, it is well accepted to use the initial unloading stiffness of the load-depth curve to determine the material's Young's modulus. This approach requires the use of high-precision displacement sensors in order to calibrate the loading apparatus system compliance and thus obtain the load-depth curve accurately. In this research, using a transparent spherical indenter coupled with a multi-partial unloading technique, we present a simpler approach to measure the material's Young's modulus. Experimental results of several metallic alloys and related discussions are presented.

Keywords Transparent indenter measurement (TIM) · Spherical indentation · Young's modulus measurement · Load-depth curve · Multi-partial unloading

Introduction

In material nano- and micro-indentation research, among all the indentation parameters, load-depth relation and unloading characteristics have been studied extensively either experimentally or numerically to elucidate the relevant mechanical behavior or properties. For example, it is well accepted to use the initial unloading stiffness of the load-depth curve to determine the material's Young's modulus [1–4]. This approach can be traced back to Sneddon's [1] classical elastic indentation solutions which describe the general relationship among the load, displacement and

contact area for any punch that can be treated as a solid of revolution of a smooth function. In the 1970s, Bulychev et al. [2] defined the initial unloading slope and reduced modulus, thus providing a theoretically sound methodology for determining the Young's modulus. This method is applicable to both spherical and pyramidal indenters. Using instrumented indentations, Doerner and Nix [3] further investigated the unloading characteristics. In 1992, Oliver and Pharr [4] showed that Bulychev's technique can be applied to any indenter that can be described as a body of revolution of a smooth function.

In the indentation research for Young's modulus measurement, the contact area and initial unloading stiffness are the key parameters to be determined. However, in most cases, direct measurement of the contact area is not applicable or not possible. Typically, the unloading stiffness is used to estimate the contact area through some iterative algorithm [5, 6]. Furthermore, high-precision displacement sensors are needed in order to accurately obtain load-depth curve and the unloading stiffness data [2–4]. As for the direct measurement of contact area, Kleesattel [7] designed a special apparatus for direct measurement of the contact region through a spherical sapphire indenter while conducting indentation tests, but the scanning method yields only one line of the contact region, and real-time access of the indented surface is not possible. By applying a special lighting technique, Frank [8] developed a transpyramidal indentation viewing system. It was also implemented by Sakaia et al. [9] using a similar technique. Recently, we have developed a Transparent Indenter Measurement (TIM) technique [15, 16]. By integrating a Twyman-Green type interferometer with the spherical transparent indenter head, the TIM system can directly measure the indentation-induced out-of-plane deformation as well as the indented surface. It was found that by using the difference of out-of-plane

C. Feng (✉, SEM member) · B.S. Kang
Mechanical and Aerospace Engineering Department,
West Virginia University,
Morgantown, WV 26506, USA
e-mail: chuanyufeng@yahoo.com

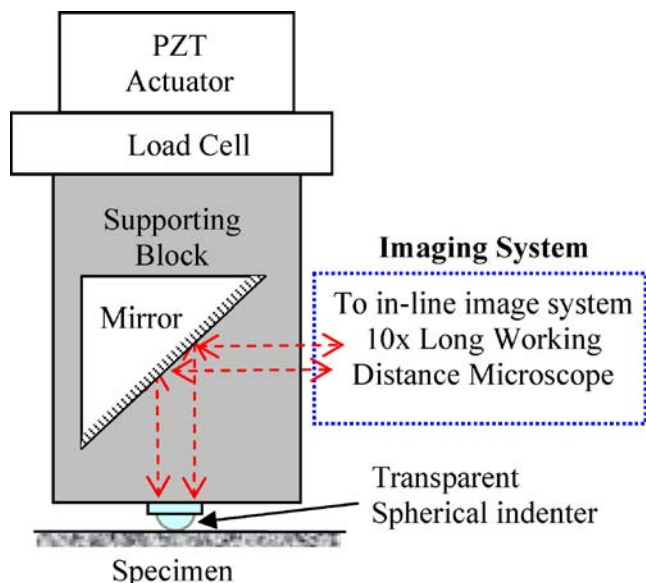


Fig. 1 Simplified transparent indenter measurement technique with in-line imaging system

deformation, Young's modulus can be evaluated without unloading stiffness measurement. Recently, a similar TIM approach was also done by Miyajima and Sakia [10] using sapphire spherical indenters on Aluminum and Zirconium oxide materials.

In this paper, we present a simplified TIM method for material's Young's modulus measurement. Compared with our previous work [15, 16], the simplified TIM method does not include interferometric optics and requires only a millimeter-size sample alloy for the indentation test, thus greatly simplifying the indentation test setup.

Theory

As shown in equation (1) [2–4], for material's Young's modulus measurement using depth-sensing indentation method, the initial unloading stiffness (dp/dh) of a load-depth curve and the contact area (A) are the key parameters to be determined. Usually, the contact area, A , is estimated indirectly from the measured unloading stiffness coupled

with iterative scheme [5, 6] or determined afterwards using microscopic methods, such as optical microscopy, SEM, AFM, etc.

$$\frac{dp}{dh} = \frac{2}{\sqrt{\pi}} E_r \sqrt{A} \quad (1)$$

where P is the indentation load, h is the indentation depth, A is the indentation contact area, E_r is the reduced modulus and $\frac{1}{E_r} = \frac{1-\nu^2}{E} + \frac{1-\nu_0^2}{E_0}$, where E is the Young's modulus, ν is Poisson's ratio of the specimen, and subscript 0 denotes the indenter's mechanical properties.

Figure 1 shows the simplified optical TIM method whereas the contact area, A , is measured directly through a transparent spherical indenter. As for the unloading stiffness (dp/dh) measurement, a closed-loop control PZT actuator is implemented in the TIM apparatus as the loading device to conduct this measurement. The PZT actuator provides high resolution displacement control (± 2 nm). However, the measured PZT tip displacement, h_{PZT} , includes both the loading system displacement, h_s , and the indentation depth, h , i.e., $h_{PZT} = h_s + h$. In terms of compliance, it can be written as

$$\frac{dh_{PZT}}{dp} = \frac{dh_s}{dp} + \frac{dh}{dp} \quad (2)$$

Substitute equation (1) into equation (2),

$$\frac{dh_{PZT}}{dp} = \frac{dh_s}{dp} + \frac{\sqrt{\pi}}{2} \frac{1}{\sqrt{A}} \frac{1}{E_r} \quad (3)$$

or

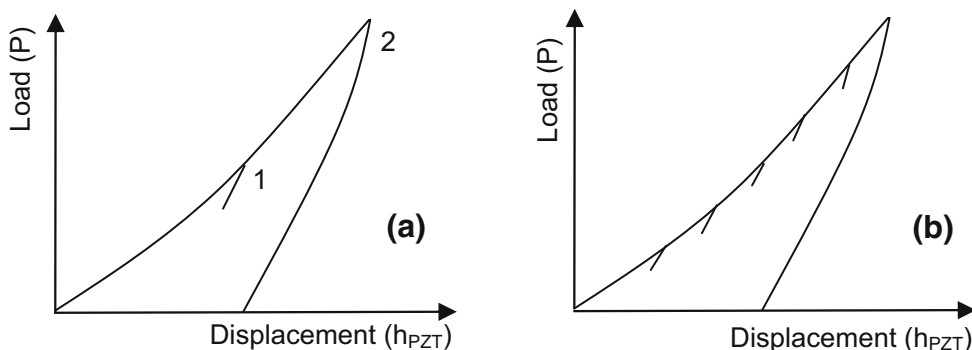
$$\frac{dh_{PZT}}{dp} = C_s + \frac{\sqrt{\pi}}{2} \frac{1}{\sqrt{A}} \frac{1}{E_r} \quad (4)$$

where $C_s = \frac{dh_s}{dp}$ is the system compliance, including the loading frame and all other components in the system.

During a simplified TIM indentation test, the system compliance (C_s) is assumed to remain constant within a proper loading range.

Under this assumption, as shown in Fig. 2(a) and based on equation (4), for a simplified TIM indentation test with

Fig. 2 Schematic load-displacement curve of a TIM indentation test. (a) With one additional partial unloading (b) With multi-partial unloadings during one indentation test



two adjacent loading/partial unloading steps, the unloading compliances for both steps 1 and 2 can be written as:

$$\frac{dh_{PZT}}{dp} \Big|_1 = C_s + \frac{\sqrt{\pi}}{2} \frac{1}{\sqrt{A_1}} \frac{1}{E_r} \quad (5)$$

$$\frac{dh_{PZT}}{dp} \Big|_2 = C_s + \frac{\sqrt{\pi}}{2} \frac{1}{\sqrt{A_2}} \frac{1}{E_r} \quad (6)$$

Subtracting equation (5) from equation (6), the system compliance is cancelled out, and the difference of unloading compliance becomes,

$$\frac{dh_{PZT}}{dp} \Big|_2 - \frac{dh_{PZT}}{dp} \Big|_1 = \frac{\sqrt{\pi}}{2} \frac{1}{E_r} \left(\frac{1}{\sqrt{A_2}} - \frac{1}{\sqrt{A_1}} \right) \quad (7)$$

Thus the reduced modulus can be calculated from equation (7):

$$E_r = \frac{\frac{\sqrt{\pi}}{2} \left(\frac{1}{\sqrt{A_2}} - \frac{1}{\sqrt{A_1}} \right)}{\frac{dh_{PZT}}{dp} \Big|_2 - \frac{dh_{PZT}}{dp} \Big|_1} \quad (8)$$

Equation (8) shows that the reduced modulus can be obtained experimentally from two partial unloading steps of a TIM indentation test. Young's modulus of the tested material can thus be determined from the reduced modulus E_r ,

$$E = \frac{1 - \nu^2}{\frac{1}{E_r} - \frac{1 - \nu_0^2}{E_0}} \quad (9)$$

This procedure can be further extended into multi-partial unloading steps, as shown in Fig. 2(b) with the corresponding in-line contact area measurement. Let's rewrite equation (4) as equation (10) such that both a (reciprocal of reduced modulus) and b (system compliance) can be obtained through linear regression.

$$\left(\frac{dh_{PZT}}{dp} \right) = \left(\frac{1}{E_r} \right) \left(\frac{\sqrt{\pi}}{2} \frac{1}{\sqrt{A}} \right) + C_s \quad (10)$$

or $y = ax + b$ where $y = \frac{dh_{PZT}}{dp}$, $a = \frac{1}{E_r}$, $x = \frac{\sqrt{\pi}}{2} \frac{1}{\sqrt{A}}$, $b = C_s$.

Equation (10) provides a convenient guideline to justify the validity of the proposed methodology, i.e., if the system compliance changes during the indentation loads, the linear relationship as depicted in equation (10) can not be maintained.

Further Discussion of System Compliance

For mechanical property measurement using instrumented nano/micro indentation technique, the effect of the system compliance is always a concern and this is why in-situ high precision and sometimes sophisticated displacement sensor is often used to remedy this problem. In this paper, we

propose a rather simple approach to try to alleviate this problem by making the assumption that within a selected loading range (of an indentation test where data are collected for mechanical property evaluation) the system compliance is constant (i.e. load versus load-line system displacement is linear within the loading range). We acknowledge that, experimentally, it is difficult to conduct direct measurement of the system compliance and thus prove the validity of this assumption. However, we noticed the investigation work of Oliver and Pharr [4] on system compliance measurement. Their approach is similar to what described in this paper, the difference is that instead of calculating the Young's modulus as proposed in this paper, it was used for system compliance determination [4]. Specifically, equation (10) shows that if the system compliance, C_s , is constant within the loading range, a plot of the measured compliance (y) versus $\frac{1}{\sqrt{A}}$ should be linear, and the intercept is the system compliance C_s . This procedure was used by Oliver and Pharr [4] for system compliance determination.

Experiments

Experimental Setup

As shown in Fig. 1, a sapphire half-spherical indenter (1.5 mm diameter in this research) is attached to a hollow stainless steel supporting block, which is then attached to a load cell and PZT actuator. A mirror is mounted inside the hollow stainless steel supporting block. An exchangeable long working distance microscope is attached to the indentation apparatus to capture the surface indentation images (i.e., the indented area, A). For the micro-indentation tests conducted in this paper, a 10× objective lens was used and through image analysis and calibration, the edge detection resolution of the indentation zone has an error of less than 0.5 μm .

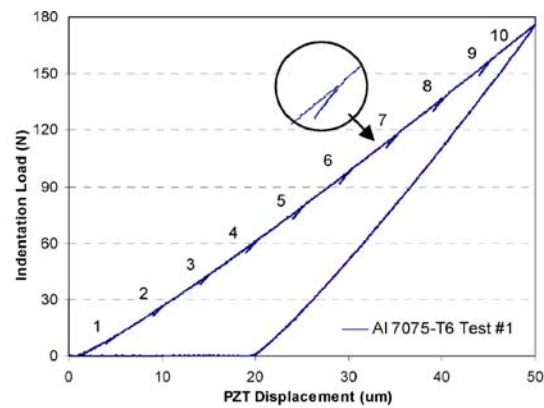
In order to run the indentation test and acquire related load-displacement data and indented area images automatically, two LabVIEW™ programs were developed. One detects the initial contact between the indenter tip and specimen, and the other controls the indentation test as well as the data and image acquisition.

Test Procedure

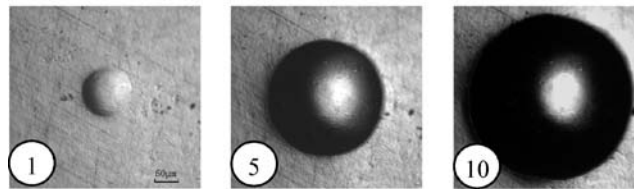
A typical TIM test involves two steps. The first step is the initial adjustment. The specimen is first attached to the specimen holder and a drop of index matching fluid is poured to fill the gap between the indenter tip and the specimen. The initial contact between the indenter and the specimen surface is established by running an initial adjustment program,

Fig. 3 Results of Al 7075-T6 indentation test. (a) Load displacement curve with multi-partial unloadings. (b) Indented surface at unloading steps 1, 5, and 10, field of view: $395\ \mu\text{m} \times 377\ \mu\text{m}$. (c) Compliance $y = \frac{dh_{PZT}}{dp}$ vs. variable

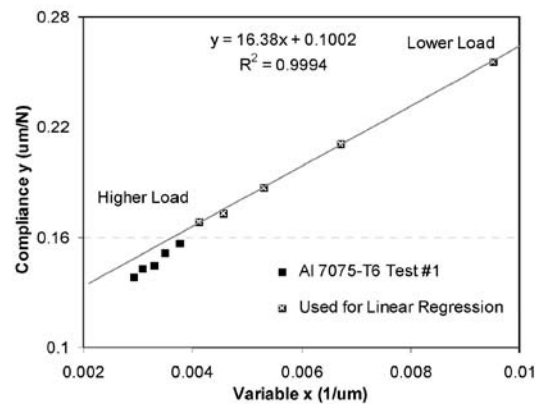
$$x = \frac{\sqrt{\pi}}{2} \frac{1}{\sqrt{A}}$$



(a)



(b)



(c)

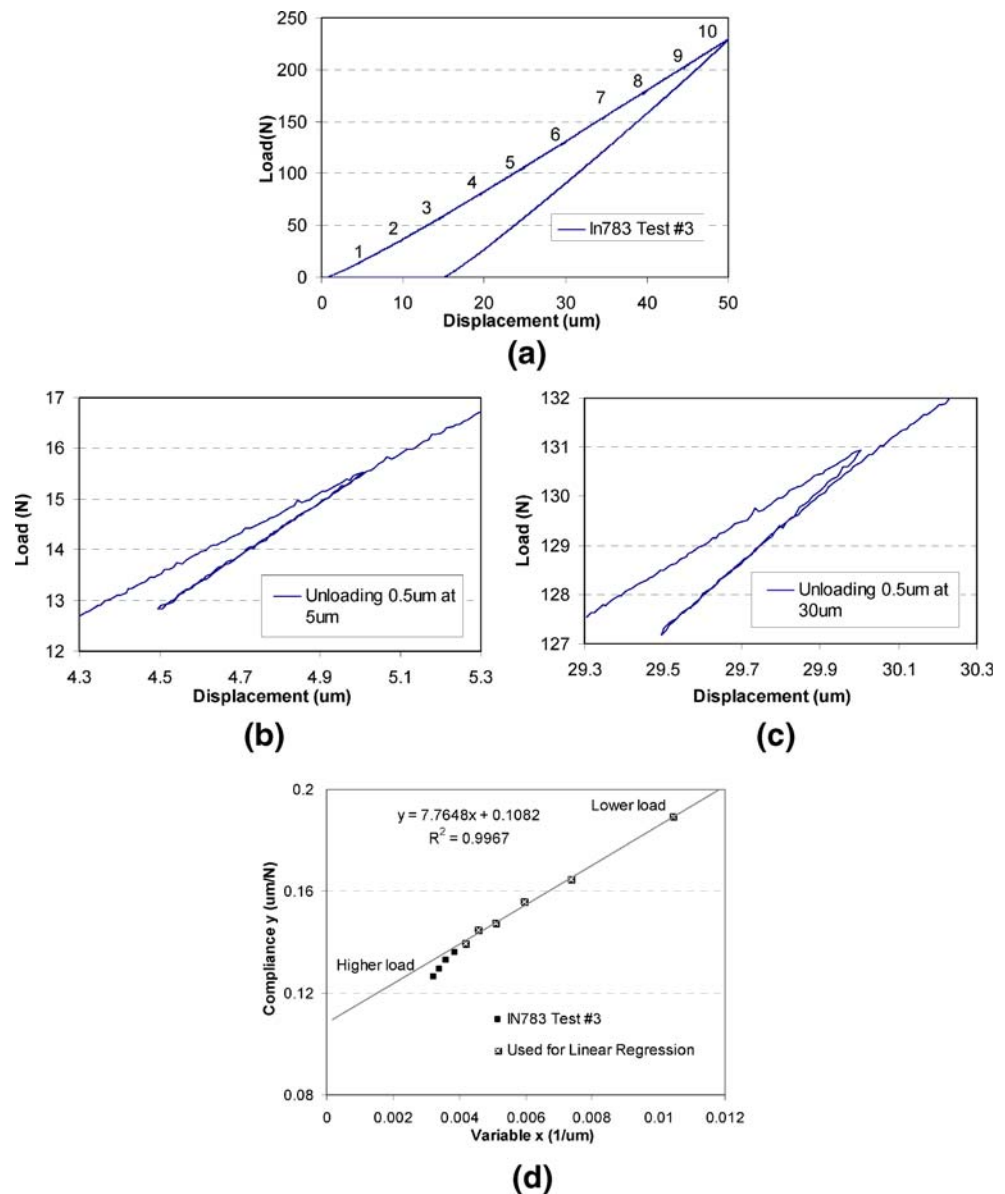
which automatically moves the indenter until it reaches the initial contact position. For this research, the initial contact criterion is set to within a certain threshold load ($\sim 0.1\ \text{N}$). When the applied load approaches the threshold load, the indenter will stop moving, record and set the initial contact position. If initial contact is to be avoided, the program can also retract the indenter to a certain distance after the initial contact has been found. After the initial contact is established, another LabVIEW™ program is used to define the indentation parameters (i.e., multi-partial unloading steps, data and image file names, velocity control, etc), and then conduct the indentation test automatically. For the results

shown in this paper, all tests were conducted with ten loading/partial unloading steps, and each partial unloading displacement was either 0.5 or $1\ \mu\text{m}$, nominally.

Table 1 Measured Young's modulus of Al 7075-T6

Test	Young's modulus (GPa)	Error (%)
#1	66.5	-7.3
#2	68.2	-4.9
#3	73.6	+2.6
#4	72.4	+0.98
#5	62.9	-12.3

Fig. 4 Results of Inconel 783 indentation test. **(a)** Load displacement curve with multi-partial unloadings. **(b)** Partial unloading/reloading at 5 μm . **(c)** Partial unloading/reloading at 30 μm . **(d)** Compliance $y = \frac{dh_{\text{PT}}}{dp}$ vs. Variable $x = \frac{\sqrt{\pi}}{2} \frac{1}{\sqrt{A}}$



Test Materials

Two alloys, Al 7075-T6 and Inconel 783 were selected for verification tests, and one research alloy Re-(26–30wt%)Cr was also investigated. The cast alloy Re-(26–30wt%)Cr was obtained from Oak Ridge National Laboratory (ORNL) as reported in [13, 14]. The published Young's modulus values for Al 7075-T6 and Inconel 783 are 71.7 and 177.3 Gpa, respectively [11, 12]. The Inconel 783 alloy had standard heat treatment (1120°C/1 h/AC+845°C/8 h/AC+720°C/8 h 50°C/h 620°C/8 h/AC). The Young's modulus of

the sapphire indenter is 340 Gpa with Poisson's ratio equal to 0.29.

Results

Al 7075-T6

Figure 3(a) shows the indentation load and displacement data. A detailed partial unloading step was inserted into Fig. 3(a) to manifest the partial unloading. Prior to each

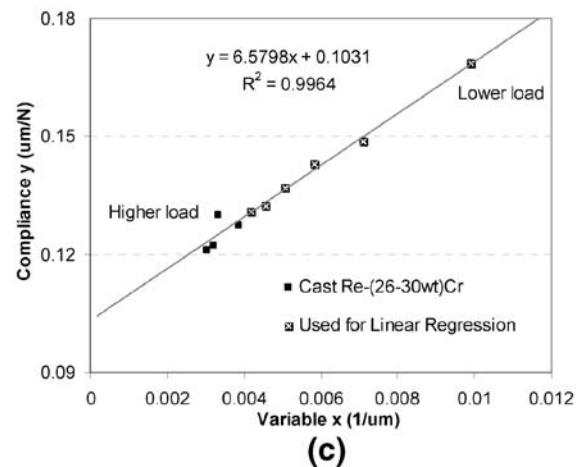
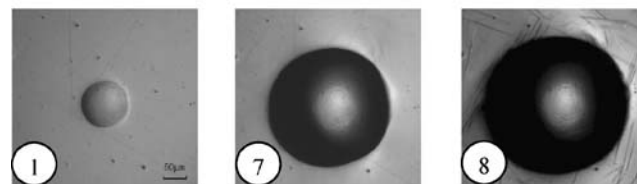
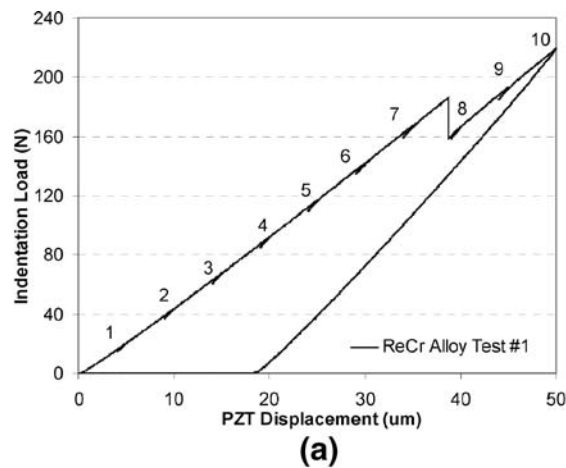
Table 2 Measured Young's modulus of Inconel 783

Test	Young's modulus (GPa)	Error (%)
#1	180.4	+1.7
#2	181.6	+2.4
#3	179.5	+1.2
#4	167.1	-5.8
#5	181.0	2.1

partial unloading, image of the indented contact zone was digitally captured in real time. Figure 3(b) shows the typical indented surface images at unloading steps 1, 5 and 10. The frame dimension for each image is 395 μm by 377 μm . Those images were then processed to obtain the contact

area at corresponding loading/unloading steps. Based on the unloading line data, compliances at each unloading step were calculated. The processed data are shown in Fig. 3(c), which shows the existence of a linear relationship within most of the applied indentation loading range. However, the data starts to deviate from the linear relationship at higher indentation loads, indicating the breakdown of the constant system compliance assumption, as discussed in the "Theory" and "Further Discussion of System Compliance" sections. Using the linear unloading line, Young's modulus was calculated by applying Equation 10 and assuming a Poisson ratio of 0.3. Table 1 summarizes the results from five indentation tests. An average value of 68.7 Gpa with a 4.4 Gpa standard deviation was obtained. The experimental data obtained are in good agreement with the book value of 71.7 Gpa.

Fig. 5 Results of cast Re-(26–30wt%)Cr indentation test. (a) Load displacement curve with multi-partial unloadings. (b) Indented surface at unloading steps 1, 7, and 8, field of view: 395 μm × 377 μm . (c) Compliance $y = \frac{dh_{PZT}}{dp}$ vs. Variable $x = \frac{\sqrt{\pi}}{2} \frac{1}{\sqrt{A}}$



Inconel 783

Test results for Inconel 783 are shown in Fig. 4. Based on the linear unloading line data [e.g. Fig. 4(b,c)], compliances were calculated. The indented surface images were processed to obtain the contact area at corresponding loading/unloading steps. Similar to the Al 7075-T6 test, a linear relationship is observed within most of indentation loads [Fig. 4(d)] and the data starts to deviate at higher indentation loads. Again, using only the linear part in Fig. 4(d), and based on equation (10), Young's modulus values were calculated. Table 2 summarizes the results for Inconel 783 from five indentation tests. An average value of 177.9 GPa with a 6.1 GPa standard deviation is obtained and agreed well with the book value of 177.3 GPa.

Re-(26–30wt%)Cr

An exploratory indentation test on a cast alloy Re-(26–30wt%)Cr [13, 14] is shown in Fig. 5. The load-depth curve shown in Fig. 5(a) clearly shows a sudden decrease of load between Steps 7 and 8. This was due to the onset of slip band formation near the surface high tensile stress region, as shown in Fig. 5(b). Due to the sudden change of the load, there is a noticeable compliance change in unloading step 8, as shown in Fig. 5(c). Using indentation data before Step 8, the Young's modulus was determined to be 234 GPa.

Conclusions

In this paper, without interferometric optics used in the original TIM technique [15, 16], a simplified TIM technique has been developed. Coupling with a multiple partial unloading testing procedure, material's Young's modulus can be determined using the simplified TIM method. Verification tests on Al 7075-T6 and Inconel 783 were conducted and the results agree well with the published values. An exploratory test of a new cast Re-(26–30wt%)Cr alloy was also conducted. Test results show the capability of the simplified TIM method to detect the sudden onset of slip bands.

It should be noted that under large loads, the system compliance may change appreciably and the proposed method to obtain the material Young's modulus may not be applicable. It is also possible that the multi-partial unload-

ings can accumulate surface microstructural damage thus lowering the Young's modulus calculation using the unloading line approach.

Acknowledgement The work is sponsored by the Office of Fossil Energy, Advanced Research Materials (ARM) Program, U.S. Department of Energy, under contract DE-AC05-00OR22725 managed by UT-Battelle, LLC.

References

1. Sneddon IN (1965) The relation between load and penetration in the axisymmetric Boussinesq problem for a punch of arbitrary profile. *Int J Eng Sci* 3:47–57.
2. Bulychev SI, Alekhin VP, Shorshorov MKh, Ternovskii AP, Shnyrev GD (1975) Determining Young's modulus from the indenter penetration diagram. *Ind Lab* 41(9):1409–1412 (Sep).
3. Doerner MF, Nix WD (1986) A method for interpreting the data from depth-sensing indentation instruments. *J Mater Res* 1(4): 601–609 (Jul/Aug).
4. Oliver WC, Pharr GM (1992) An improved technique for determining hardness and elastic modulus using load and displacement sensing indentation experiments. *J Mater Res* 7(6): 1564–1583 (June).
5. Taljat B, Zacharia T (1998) New analytical procedure to determine stress-strain curve from spherical indentation data. *Int J Solids Struct* 35(33):4411–4426.
6. Haggag FM (1989) Field indentation microprobe for structural integrity evaluation, U.S. patent no. 4,852,397, August 1.
7. Kleesattel C (1981) Method and apparatus for the measurement of hardness testing indentations. U.S. patent no. 4,277,174, July 7.
8. Frank S (2000) Transpyramidal indentation viewing—new possibilities for mobile hardness testing. In: 15th world conference on non-destructive testing, Rome, October.
9. Sakaia M, Hakiri N, and Miyajima T (2006) Instrumented indentation microscope: A powerful tool for the mechanical characterization in microscales. *J Mater Res* 21(9):2298–2303 (Sep).
10. Miyajima T, and Sakaia M (2006) Optical indentation microscopy—a new family of instrumented indentation testing. *Philos Mag* 86 (33–35):5729–5737 (21 Nov–11 Dec).
11. POC Company. IN783 mechanical properties. <http://www.special-metals.com>.
12. MatWeb. Al 7075-T6 mechanical properties. <http://www.matweb.com>.
13. Brady MP, Anderson IM, Weaver ML, Meyer HM, Walker LR, Miller MK, Larson DJ, Wright IG, Sikka VK, Rar A, Pharr GM, Keiser JR, and Walls CA (2003) Nitrogen impurity gettering in oxide dispersion ductilized chromium. *Mater Sci Eng A* 358(1–2):243–254.
14. Ma N, Cooper BR, and Kang BS (2006) Tight-binding study of thermal expansions for Mo3Si. *J Appl Phys* 99:053514.
15. Chuanyu F (2005) Development of a transparent indenter measurement system and indentation analysis for material mechanical properties evaluation. Dissertation, West Virginia University, 2005.
16. Feng C, Kang BS (2006) A transparent indenter measurement method for mechanical property evaluation. *Exp Mech* 46(1):91–103 (Feb).